UDC 004.056.55

MATHEMATICAL MODEL AND METHODS OF PROCESSING BIOMETRIC IMAGES OF FINGERPRINTS

Emiliia Anishchenko, Serghii Rassomakhin

V. N. Karazin Kharkiv National University, 6 Svobody Sq., Kharkiv, 61022, Ukraine
emily9661@gmail.com, rassomakhin@karazin.ua

Reviewer: Vyacheslav Kharchenko, Doctor of Technical Sciences, Prof., Academician of the Academy of Sciences of Applied Radio Electronics, National Aerospace University named after. M. E. Zhukovsky, Kharkiv, Ukraine.
E-mail: v_s_kharchenko@ukr.net

Received on June 2018

Abstract: *Today, using of personal identification technologies based on biometric parameters for access to information resources is becoming topical in connection with the increase of informatization in modern society. Physical characteristics such as face, voice, retina or fingerprints are used to confirm personal identity. The most successful biometric identification technology is fingerprinting - a comparison of fingerprints. It is easy for using, reliable and there is no outside intrusion. The article will consider an analytical probabilistic model of formation and processing of fingerprints portraits taking into account possible natural factors that can distort the image of prints. Also, the model was processed to minimize the distortions' influence to approximate the distribution type of characteristic points to a similar distribution of the reference sample.*

Keywords: *biometry; model; methods; fingerprints.*

1 Introduction

Personal identification using of fingerprinting is a promising developing direction. Biometric information is unique, it can not be forgotten or lost. The presentation of information requires the physical personal presence. The method uses the uniqueness of the pattern of papillary patterns on the fingers of people.

The imprint obtained using the scanner converts into a digital code and then compares with previously entered sets of standards. Obtaining an electronic fingerprint with a clearly visible papillary pattern is a difficult task. The fingerprint is too small, it is necessary to use various methods to obtain its high-quality image. A lot of external factors can distort the patterns of prints during scanning the finger.

Today, all biometric technologies are probabilistic and none of them can guarantee the complete absence of errors.

The advantages of the fingerprint identification method are:

• The uniqueness of fingerprints. They are unique from each other as well as other fingerprints of any person. Even twins have fingerprints that are different.

• It is impossible to lose or forget fingerprints, as with passwords or PIN codes.

• Fingerprints do not change over time.

• Fingerprints have been used for many years to identify individuals. Therefore, it is possible to approve the developed algorithms using existing databases.

In each fingerprint you can define two types of signs - global and local. Global signs – fingerprint characteristics that you can see easily. Global signs include the image region, the core, the "delta" point, the line counter, the papillary pattern. Local signs called Minutiae are small unique points for each fingerprint, which are used to identify the individual. A fingerprint may have the same global signs but local signs are always unique. Therefore, the process of individual identification usually consists of two stages. The first step is the classification of fingerprints on global grounds using the databases for the division into classes and at the phase of authentication. The second stage is the fingerprint recognition (*identification*) on the comparison basis of the structure and coincidence coefficient of minutiae points.

2 Principle of fingerprint recognition

Depending on the obtained image of fingerprints quality we can identify some fingers surface characteristic features, which can later be used for identification purposes. If the image resolution obtained from the scanner is 300–500 dpi, a sufficiently large number of small details (*minutiaes*) can be distinguished in the fingerprint image. They can be divided into two automated types: end-points - points where papillary lines finish; and branch points - points where the papillary lines split into two. In Fig. 1 is an example showing endpoints and branch points.

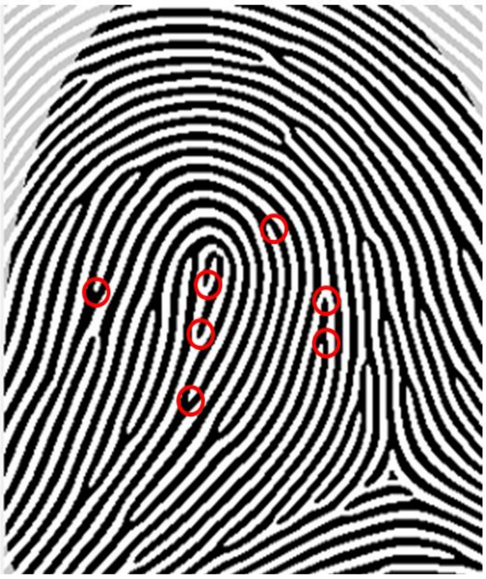

Fig. 1 - Endpoints and branch points

The fingerprint identification principle depends on the presence of the special points on the print - minutiaes. Each minutiae conditionally has own coordinates, direction and type (ending, branching, etc.). When algoritm has a set of singular points {(X, Y, θ, type), which were retrieved during registration it evaluates the point samples similarity and gives the result – "Identified" or "Not recognized". In the task of identification / verification of a person by fingerprint, the following three main stages can be distinguished which are modern algorithms characteristic:

1) processing of the original image;
2) isolation of minutiaes;
3) comparison of minutiaes' fingerprints.

As a rule, if it is not received electronically the fingerprint original image has bad quality (*lines are damaged, there are different distortions, etc.*).

The distortion types and distribution functions are not simple because of the causes multiple nature. All existing fingerprint recognition algorithms are closed for access, so there is no possibility to study the placement statistics and minutiaes distortion which would be sufficient for a clear problem solution. Therefore, the models presented below were obtained on the scanning processes heuristic analysis basis taking into account the possible errors nature.

3 Mathematical model of fingerprints characteristic points distribution

To develop an obtaining high-entropy data method based on various biometric images implementations the model has to describe the minutiae random distribution and arrival angles as well as the error realizations random distribution. According to the minutiae distribution portraits analysis the following *features* can be noted:

- point distribution density along the horizontal (X) and vertical (Y) axis has an approximately level character in the frame central part and slightly decreases to its edges;

- fingerprint center linear displacements on the horizontal and vertical do not mean the appearance of free from minuciae zones at the edges of the frame (*new points can get into the scanning field*);

- "arrival angles" distribution at characteristic points is approximately level in the range $[0,\ 2\pi]$.

To build a minuciae distribution model we will assume that:

- fingerprint portrait coordinates X, Y as well as the arrival angles values are normalized in the range [-0.5; +0.5], while the image geometric center has coordinates [0;0]. The portrait is placed in a unit square area covering all image plane;

- for the initial random numbers generation required to obtain the minutiaes coordinates on fingerprints implementations we use the sensor with uniformly distributed (*continuously*) numbers in the range [0;1]: $f(x_i, y_i) \sim \text{unif}[0,1]$, $i \in 1 \ldots N$ where N is the number of minutiaes in the portrait –

random value in the range with [15; 60] with mathematical expectation $m_N = 25 \div 35$ and unimodal distribution.

Therefore, we can use the dependence shown in Fig. 2 for the formal *probability distribution density* (PDD) description f(x) and f(y).

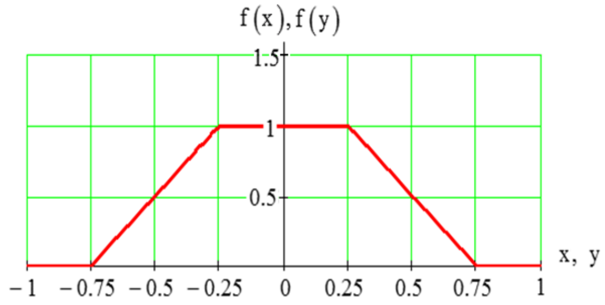

Fig. 2 – The minutiae coordinates probability density functions

To obtain minutiaes placement portraits test samples we need a random numbers source, distributed in accordance with the PDD (Fig. 2). Due to the distributions identity along the plane coordinates using the normalized unit portrait square in the future we will use only the function:

$$f(x) = \begin{cases} 2x + 1.5 & \text{if } -0.75 \le x < -0.25; \\ 1 & \text{if } -0.25 \le x \le 0.25; \\ -2x + 1.5 & \text{if } 0.25 < x \le 0.75; \\ 0 & \text{if } |x| > 0.75. \end{cases} \quad (1)$$

Using the inverse functions method:

if $z \sim \text{unif}[0,1]$ then a random variable x obtained by a functional transformation z of the form

$$x = \begin{cases} \sqrt{z} - 0.75 & \text{if } 0 \le z < 0.25; \\ z - 0.5 & \text{if } 0.25 \le z \le 0.75; \\ -\sqrt{1-z} + 0.75 & \text{if } 0.75 < z \le 1; \end{cases} \quad (2)$$

will have PDD (1).

Fig. 3 shows the functional transformation (2) statistical test histogram with the experiments equal number to 30,000 and the interval division [-0.75; +0.75] into 100 equal subintervals. The dashed line in fig. 3 shows the envelope line (1).

The generating random numbers resulting algorithm will be used in the future to obtain the prints normalized square portraits characteristic points coordinates.

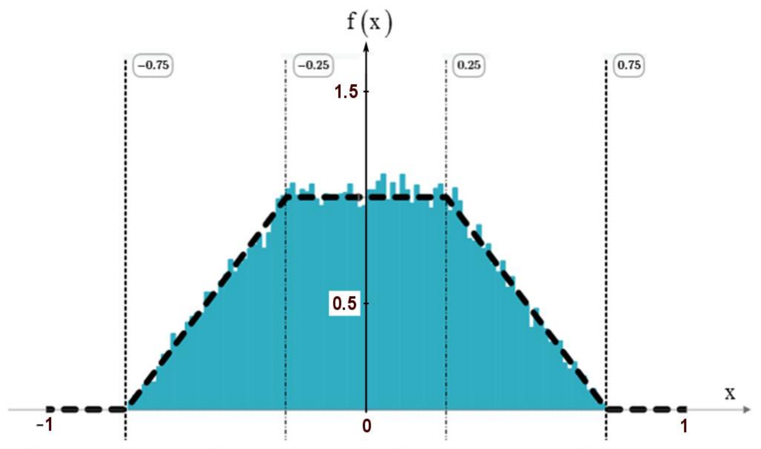

Fig. 3 – The sensor random coordinates statistical tests result

To generate a random number of characteristic points for the print portrait implementation we use discrete (integer) random variable model N: [15, 45] with a discrete normal truncated distribution and numerical characteristics:

- expectation $m_N \approx 30$;

- standard deviation $\sigma \approx 2 \div 5$.

To obtain a minutiae random number on the portrait implementation N, we use the unif[0,1] functional data transformation. We proceed to the uniformly distributed numbers discrete form using the integer rounding and centering operation:

$$z' = \text{round}(z) - 0.5, \text{ where } z \sim \text{unif}\,[0,1]. \quad (3)$$

Then, with limit to the number of terms equal to $m_N = 30$ the minutiae random number in the portrait can be defined as the sum

$$N=\sum_{i=1}^{30} z' + 30 \tag{4}$$

A discrete random variable can take integer values from a range [15, 45]. Than the truncated normal function of the PDD:

$$Q(N_i)=\binom{i}{30}\cdot\left(\frac{1}{2}\right)^{30}, \quad i\in[0,30],\ N_i\in[15,45] \tag{5}$$

Where $Q(N_i)$ is the probability that the minutes number in a portrait (taking into account the points masked outside the unit square) will be N_i.

The distribution type and numerical characteristics (5) are shown in fig. 4.

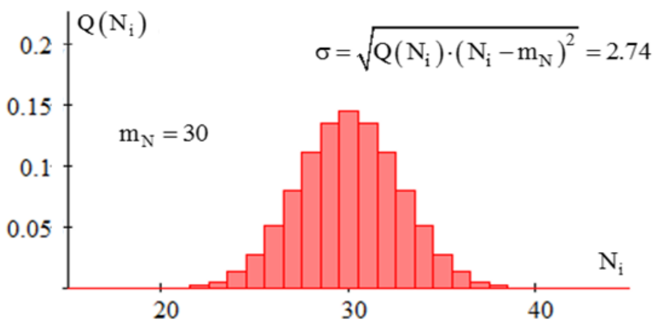

Fig. 4 – PDD normalized print portrait of the characteristic points number

To simulate the arrival angles random values normalized in a unit square at characteristic points, we use a random variable z ~ unif [0,1] uniformly distributed over a single segment:

$$\varphi = z. \tag{6}$$

The true arrival angle is determined based on the normalized value (6): $\Phi = 2\pi\cdot\varphi$.

Table 1 presents the normalized portrait simulation results based on the distributions (1), (4) and (6).

Table 1 - Portrait Matrix

№	X	Y	φ
1	0.21	-0.07	0.6
2	0.28	0.18	0.58
3	0.12	-0	0.49
4	0.19	0.31	0.74
5	0.07	-0.68	0.62
6	0.05	-0.12	0.8
7	-0.25	0.33	0.58
8	-0.01	0.42	0.91
9	0.17	0.15	0.73
10	0.12	0.23	0.67

4 Mathematical model of the characteristic point distortion

We can list the main factors that lead to differences in fingerprint image implementations:

- geometric center displacements, caused by a change with the object position in the scanning field;
- images rotation arising for the same reasons;
- "erasure" or the appearance of "false" points due to scanner algorithm incorrect settings or the foreign objects entry in the scanning field;
- points relative position drift due to errors in the recognition algorithm.

Geometric center displacement errors

To describe such errors distribution we use a PDD with a form (1) with a horizontally modified scale:

$$\Phi(d_y),\Phi(d_x)=\begin{cases}12.5\cdot d_x+3.75 & \text{if } -0.3\le d_x<-0.1;\\ 2.5 & \text{if } -0.1\le d_x\le 0.1;\\ -12.5d_x+3.75 & \text{if } 0.1<d_x\le 0.3;\\ 0 & \text{if } |d_x|>0.3.\end{cases} \tag{7}$$

If z ~ unif [0,1], then for obtaining a random variable with distribution (7) we have to use the transformation:

$$d_x(z)=\begin{cases}\sqrt{0.16\cdot z}-0.3 & \text{if } 0\le z<0.25;\\ 0.4\cdot z-0.2 & \text{if } 0.25\le z\le 0.75;\\ -\sqrt{0.16\cdot(1-z)}+0.3 & \text{if } 0.75<z\le 1.\end{cases} \tag{8}$$

Errors due to "erasure" and adding "false" points

Assuming erasure errors independence distribution is described by the usual discrete binomial distribution:

$$P_E(k) = \sum_{i=0}^{k} \binom{i}{N} \cdot p_E{}^{i} \cdot (1 - p_E)^{N-i} \tag{9}$$

Where $P_E(k)$- the probability of erasure no more than points in the portrait; N - the identified points number, determined by the distribution (5).

We generate a vector $Z = \{z_1, z_2, \cdots, z_N\}$. Based on the vector Z we calculate the erase vector the elements of which have a binary value and are obtained by a vector Z coordinates functional transformation:

$$e_i = \left\lfloor \frac{z_i}{1 - p_E} \right\rfloor, \quad e_i = [0,1], \; i = 1 \ldots N \tag{10}$$

A probabilistic errors description associated with the false points appearance can be made on the Poisson distribution basis:

$$\Pr(K) = \frac{\lambda_A{}^{K}}{K!} e^{-\lambda_A}, \tag{11}$$

where Pr (K) is the false point appearance probability on the portrait implementation; λ_A – (Appearance) false point number empirically determined expectation in one portrait.

The approximation of random variable – the false points number in a portrait (11) is achieved using a sensor unif [0,1] and a usual binomial distribution as follows: an expectation is determined empirically by the false points number in one portrait λ_A: $0.1 \le \lambda_A \le 0.5$. A vector $Z = \{z_1, z_2, \cdots, z_M\}$ is generated with elements uniformly distributed in a unit interval z ~ unif [0,1]. Then, on the transformation basis similar to (10), we get an adding vector with binary elements obtained by the rule:

$$a_i = \left\lfloor \frac{z_i}{1 - \frac{\lambda_A}{M}} \right\rfloor, \quad a_i = [0,1], \; i = 1 \ldots M. \tag{12}$$

The square length of the vector determines the false point number added to the portrait:

$$K = |A|^2 = \sum_{i=1}^{M} a_i. \tag{13}$$

The Poisson distribution approximation (11) will be more exact if the selected value M will be larger. For an acceptable approximation it suffices to require the inequality fulfillment of:

$$M \ge \lambda^{-1}. \tag{14}$$

Image rotation errors

The relationship between the arbitrary point coordinates $\binom{X}{Y}$ in the original coordinate system XOY and the new point coordinates $\binom{X'}{Y'}$ in the system X′OY′ deployed at an angle α is specified in matrix form with the following expression:

$$\begin{pmatrix} X' \\ Y' \end{pmatrix} = U(\alpha) \cdot \begin{pmatrix} X \\ Y \end{pmatrix}, \text{ where } U(\alpha) = \begin{pmatrix} \cos\alpha & \sin\alpha \\ -\sin\alpha & \cos\alpha \end{pmatrix}. \tag{15}$$

The portrait points' location rotation by an angle is achieved by converting the submatrix:

$$XY' = U(-\alpha) \cdot (XY)^T, \tag{16}$$

where $(XY)^T$ is the transposed submatrix XY.

The change in the vector associated with the rotation of the portrait is determined by the formula:

$$\varphi' = \left(\varphi - \frac{\alpha}{2\cdot\pi}\right)\mathrm{mod}1 - \left\lfloor \left(\varphi - \frac{\alpha}{2\cdot\pi}\right)\mathrm{mod}1 \right\rfloor, \tag{17}$$

where the operation extracts the fractional part from 'arg' taking into account a sign.

The matrix of the portrait turned to the angle α is determined with the submatrices and the vector union:

$$G' = \left(\left(XY'\right)^T \| \varphi'\right). \tag{18}$$

Image rotation errors are defined by the random rotation angle distribution. Empirical considerations allow to limit the range of possible values within the right angle

$$\alpha \in \left[-\frac{\pi}{4}, +\frac{\pi}{4}\right]. \tag{19}$$

The rotation random normalized angle implementation is obtained by a functional transformation of the form:

$$\alpha_H = \sum_{i=1}^{4}\left(\frac{z_i - 0.5}{16}\right). \tag{20}$$

Approximate normal PDD is:

$$f(\alpha_H) = \frac{1}{\sqrt{2\pi}\sigma}\exp\left(-\frac{\alpha_H{}^2}{2\sigma^2}\right), \quad \sigma = \sqrt{\frac{1}{3\cdot 256}}. \tag{21}$$

Fig. 5 shows the function form (21) (*dashed line*) and the approximation probability distribution histogram (20), obtained with the 10^5 tests. As we can see, using only four terms in the sum expression (20) provides a normal PDD approximation.

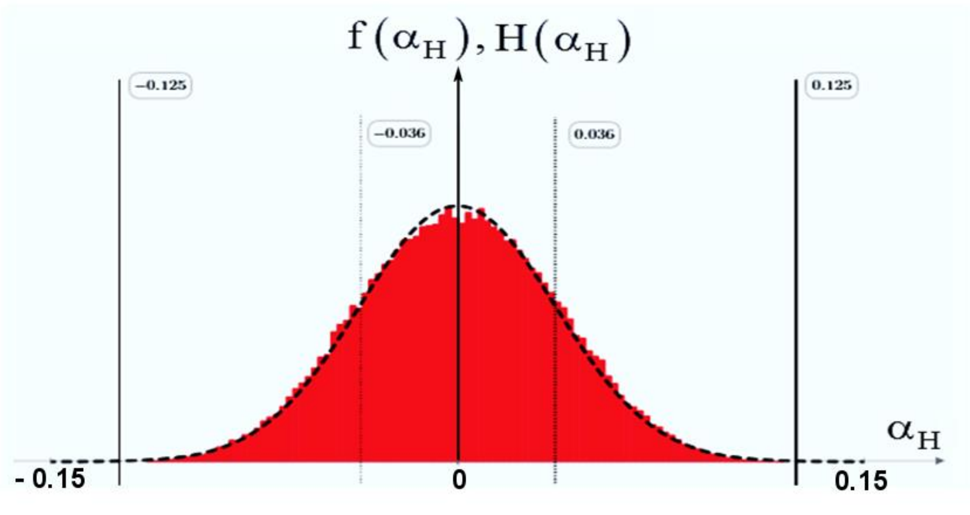

Fig. 5 – The PDD and the rotation normalized random angle PDD approximation histogram

5 Getting the original model portrait in the normalized unit square

The portrait implementation generation is performed with using the obtained functional transformations of a random variable uniformly distributed in a unit interval.

Determine the detected characteristic points. Using a software sensor with uniformly distributed numbers we get a vector of 15 elements: Z={z_1, z_2,…, z_{15}}, where $z_i \sim$ unif[0,1].

Table 2 – Z

№	z_i	№	z_i	№	z_i
1	0.001	6	0.174	11	0.989
2	0.193	7	0.71	12	0.119
3	0.585	8	0.304	13	0.009
4	0.35	9	0.091	14	0.532
5	0.823	10	0.147	15	0.602

Table 3 – Z'

№	z_i'	№	z_i'	№	z_i'
1	-0.5	6	-0.5	11	0.5
2	-0.5	7	0.5	12	-0.5
3	0.5	8	-0.5	13	-0.5
4	-0.5	9	-0.5	14	0.5
5	0.5	10	-0.5	15	0.5

Using the transformation (3) go to the vector containing the centered binary elements: $Z' = \mathrm{round}(Z) - 0.5$.

Applying the transform (4) using elements z_i' gives a random number of minutes:

$$N = \sum_{1}^{15} z' + 15 = 16 .$$

For random coordinates generating of points on a plane we use the sensor unif[0,1] and get two vectors (Tables 4 and 5) which contains random numbers from the range [0,1]:

$$Z^1 = \left\{z_1^1, z_2^1, \cdots, z_N^1\right\}, \quad Z^2 = \left\{z_1^2, z_2^2, \cdots, z_N^2\right\}.$$

Table 4 – Z^1

№	z_i^1	№	z_i^1
1	0.376	9	0.458
2	0.677	10	0.744
3	0.009	11	0.599
4	0.276	12	0.735
5	0.588	13	0.572
6	0.838	14	0.152
7	0.485	15	0.425
8	0.744	16	0.517

Table 5 – Z^2

№	z_i^2	№	z_i^2
1	0.28	9	0.55
2	0.682	10	0.472
3	0.722	11	0.847
4	0.123	12	0.456
5	0.835	13	0.983
6	0.517	14	0.739
7	0.426	15	0.196
8	0.949	16	0.839

Applying the transformation (2) to the tables 4 and 5 elements we obtain two coordinate vectors:

Table 6 – X

№	x_i	№	x_i
1	-0.124	9	-0.042
2	0.177	10	0.244
3	-0.656	11	0.099
4	-0.224	12	0.235
5	0.088	13	0.072
6	0.347	14	-0.361
7	-0.015	15	-0.075
8	0.244	16	0.017

Table 7 – Y

№	y_i	№	y_i
1	-0.22	9	0.05
2	0.182	10	-0.028
3	0.222	11	0.359
4	-0.399	12	-0.044
5	0.343	13	0.619
6	0.017	14	0.239
7	-0.074	15	-0.307
8	0.525	16	0.349

Simulating the normalized arrival angles values in the minutiaes we use unif [0,1] and get the vector φ (Table 8):

Table 8 – φ

№	φ_i	№	φ_i	№	φ_i	№	φ_i
1	0.806	5	0.752	9	0.437	13	0.696
2	0.211	6	0.543	10	0.578	14	0.19
3	0.553	7	0.437	11	0.629	15	0.178
4	0.114	8	0.696	12	0.504	16	0.457

The portrait characteristics combined matrix (Table 9) is obtained by vectors augmentation specified by tables 6–8:

$$G = \left(X \| Y \| \varphi \right). \tag{22}$$

Table 9 – G

№	$G^X{}_i$	$G^Y{}_i$	$G^\varphi{}_i$	№	$G^X{}_i$	$G^Y{}_i$	$G^\varphi{}_i$
1	-0.124	-0.22	0.806	9	-0.042	0.05	0.437
2	0.177	0.182	0.211	10	0.244	-0.028	0.578
3	-0.656	0.222	0.553	11	0.099	0.359	0.629
4	-0.224	-0.399	0.114	12	0.235	-0.044	0.504
5	0.088	0.343	0.752	13	0.072	0.619	0.696
6	0.347	0.017	0.543	14	-0.361	0.239	0.19
7	-0.015	-0.074	0.437	15	-0.075	-0.307	0.178
8	0.244	0.525	0.696	16	0.017	0.349	0.457

The shaded lines in table 9 correspond to points that did not fit in the unit square. In Fig. 6 the points defined by these rows of the matrix G are “masked” in the planar portrait.

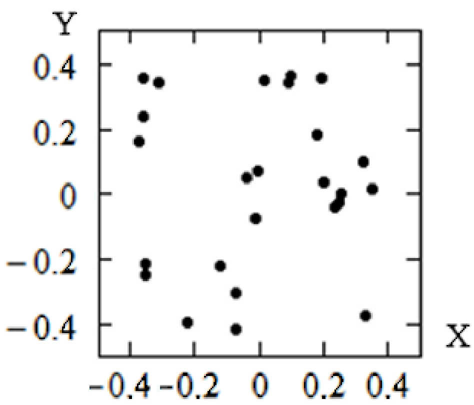

Fig. 6 – Planar portrait G

6 Example of portrait geometric center displacement implementation

To simulate the portrait geometric center displacement error defined by the matrix from table 9 we obtain a random vector of 2 elements using the sensor [0,1]:

$$Z = \begin{pmatrix} z_1 \\ z_2 \end{pmatrix} = \begin{pmatrix} 0.494 \\ 0.741 \end{pmatrix}. \tag{23}$$

Using the elements functional transformation (8) we proceed to the displacement values along the coordinates X and Y which distribution is subordinated to the centered trapezoidal function of the PDD (7):

$$d_X = d\left(z_1\right) = -0.002; \quad d_Y = d\left(z_2\right) = 0.096. \tag{24}$$

Then the following association will determine the displacement matrix:

$$Gd = \left(X + d_X \| Y + d_Y \| \varphi \right) = \left(Gd^X \| G\,d^Y \| Gd^\varphi \right). \tag{25}$$

The matrix and the corresponding portrait will have the form presented in table 10 and Fig. 7.

Table 10 – Gd

№	$Gd^X{}_i$	$Gd^Y{}_i$	$Gd^\varphi{}_i$	№	$Gd^X{}_i$	$Gd^Y{}_i$	$Gd^\varphi{}_i$
1	-0.126	-0.124	0.806	9	-0.044	0.146	0.437
2	0.175	0.279	0.211	10	0.242	0.068	0.578
3	-0.658	0.318	0.553	11	0.097	0.455	0.629
4	-0.226	-0.303	0.114	12	0.233	0.052	0.504
5	0.086	0.44	0.752	13	0.07	0.716	0.696
6	0.345	0.113	0.543	14	-0.363	0.335	0.19
7	-0.017	0.023	0.437	15	-0.077	-0.211	0.178
8	0.242	0.621	0.696	16	0.015	0.446	0.457

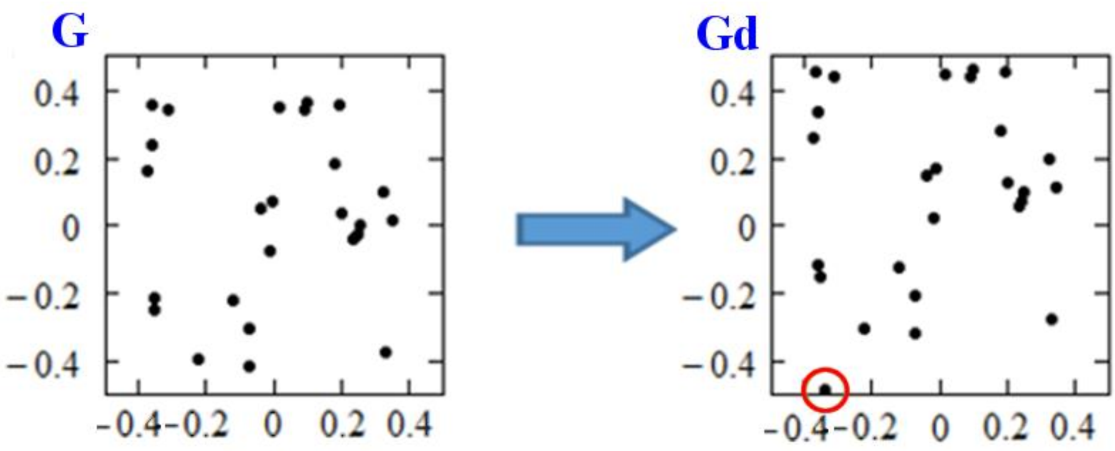

Fig. 7 – Original and displaced fingerprint portraits

However, the type of portrait is not final, because it is also can have the errors of random rotation and "erase-add".

7 Distorted portrait model converting

Make the following overrides:

- $G = Gctn$ - reference portrait is centered, truncated and normalized by the fingerprint rotation angle;
- $GD = Gd\alpha ea$ - portrait implementation distorted with random errors.

Matrix GDe consists the data about 27 portrait points.

Table 11 – GDe

№	$GDe^X{}_i$	$GDe^Y{}_i$	$GDe^\varphi{}_i$	№	$GDe^X{}_i$	$GDe^Y{}_i$	$GDe^\varphi{}_i$	№	$GDe^X{}_i$	$GDe^Y{}_i$	$GDe^\varphi{}_i$
1	-0.075	-0.161	0.863	11	-0.458	0.187	0.247	21	0.403	-0.147	0.682
2	0.066	0.322	0.268	12	0.002	-0.225	0.235	22	-0.449	0.301	0.623
3	-0.106	-0.363	0.171	13	-0.142	0.423	0.514	23	0.231	0.296	0.241
4	-0.074	0.442	0.809	14	0.199	0.178	0.155	24	-0.282	-0.267	0.612
5	0.283	0.227	0.6	15	-0.069	0.155	0.989	25	0.43	-0.494	0.3
6	-0.024	0.015	0.494	16	0.14	0.189	0.952	26	0.208	-0.387	0.722
7	-0.093	0.121	0.494	17	-0.441	0.106	0.468	27	-0.284	0.382	0.015
8	0.203	0.149	0.635	18	0.021	0.487	0.685	-	-	-	-
9	-0.069	0.46	0.686	19	0.042	-0.328	0.509	-	-	-	-
10	0.2	0.131	0.561	20	-0.297	-0.237	0.912	-	-	-	-

Centering portrait implementation

We calculate the mass center coordinates for the matrix GDe using the first two columns data:

$$\overline{Xe} = \frac{1}{Ne}\sum_{i=1}^{Ne} GDe^X{}_i \approx -0.016, \ \overline{Ye} = \frac{1}{Ne}\sum_{i=1}^{Ne} GDe^Y{}_i \approx 0.073. \tag{26}$$

Conversion GDe by centering gives:

$$GDec = \left(GDe^X - \overline{Xe} \| GDe^Y - \overline{Ye} \| GDe^\varphi\right) = \left(GDec^X \| GDec^Y \| GDec^\varphi\right). \tag{27}$$

Fig. 8 shows the obtained result by comparing the two portraits and we can see the resulting matrix in the Table 12.

One of the points left the unit normalized square limits and became one of the masked part.

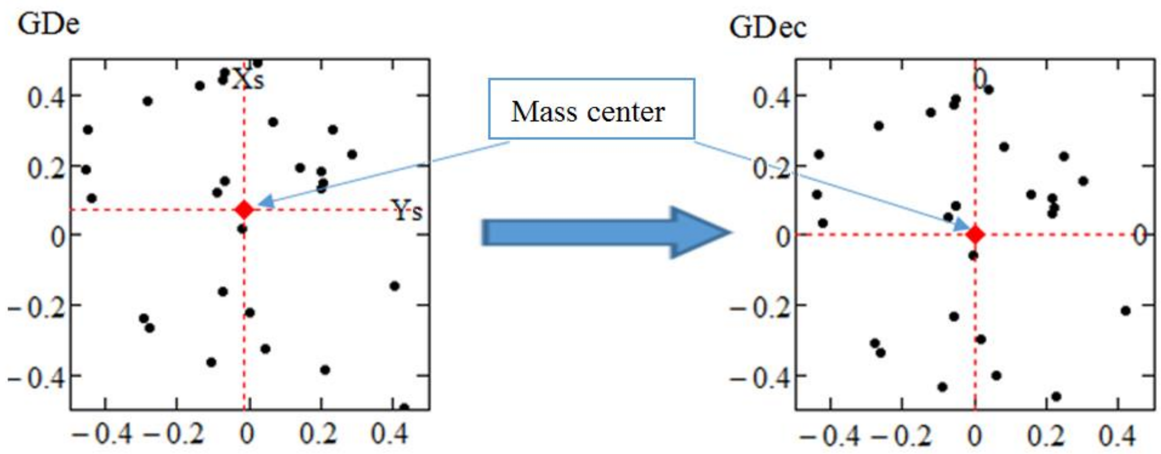

Fig. 8 – Transform portrait implementation after centering

Table 12 – Gdec

№	$GDec^{X}_{i}$	$GDec^{Y}_{i}$	$GDec^{\varphi}_{i}$	№	$GDec^{X}_{i}$	$GDec^{Y}_{i}$	$GDec^{\varphi}_{i}$	№	$GDec^{X}_{i}$	$GDec^{Y}_{i}$	$GDec^{\varphi}_{i}$
1	-0.059	-0.233	0.863	11	-0.441	0.114	0.247	21	0.419	-0.22	0.682
2	0.082	0.25	0.268	12	0.018	-0.297	0.235	22	-0.433	0.229	0.623
3	-0.09	-0.436	0.171	13	-0.126	0.35	0.514	23	0.247	0.224	0.241
4	-0.058	0.369	0.809	14	0.215	0.106	0.155	24	-0.266	-0.34	0.612
5	0.299	0.154	0.6	15	-0.053	0.082	0.989	25	0.446	-0.567	0.3
6	-0.008	-0.058	0.494	16	0.156	0.116	0.952	26	0.224	-0.46	0.722
7	-0.077	0.048	0.494	17	-0.425	0.033	0.468	27	-0.268	0.309	0.015
8	0.219	0.076	0.635	18	0.037	0.415	0.685	-	-	-	-
9	-0.053	0.387	0.686	19	0.058	-0.401	0.509	-	-	-	-
10	0.216	0.058	0.561	20	-0.281	-0.309	0.912	-	-	-	-

The truncation of points plurality in the portrait

We arrange the portrait matrix rows according to the points remoteness degree from the geometric center combined with the mass center. Calculate the points distance from the center

$$RD_i = \sqrt{\left(GDec_{i,0}\right)^2 + \left(GDec_{i,1}\right)^2}, \quad i = 1, \cdots, Ne. \tag{28}$$

Sorting rows according to values (28) gives the following matrix:

Table 13 – Gdecs

№	$GDecs^{X}_{i}$	$GDecs^{Y}_{i}$	$GDecs^{\varphi}_{i}$	№	$GDecs^{X}_{i}$	$GDecs^{Y}_{i}$	$GDecs^{\varphi}_{i}$	№	$GDecs^{X}_{i}$	$GDecs^{Y}_{i}$	$GDecs^{\varphi}_{i}$
1	-0.008	-0.058	0.494	11	0.247	0.224	0.241	21	-0.266	-0.34	0.612
2	-0.077	0.048	0.494	12	0.299	0.154	0.6	22	-0.09	-0.436	0.171
3	-0.053	0.082	0.989	13	-0.126	0.35	0.514	23	-0.441	0.114	0.247
4	0.156	0.116	0.952	14	-0.058	0.369	0.809	24	0.419	-0.22	0.682
5	0.216	0.058	0.561	15	-0.053	0.387	0.686	25	-0.433	0.229	0.623
6	0.219	0.076	0.635	16	0.058	-0.401	0.509	26	0.224	-0.46	0.722
7	0.215	0.106	0.155	17	-0.268	0.309	0.015	27	0.446	-0.567	0.3
8	-0.059	-0.233	0.863	18	0.037	0.415	0.685	-	-	-	-
9	0.082	0.25	0.268	19	-0.281	-0.309	0.912	-	-	-	-
10	0.018	-0.297	0.235	20	-0.425	0.033	0.468	-	-	-	-

Except points with numbers 17 – 27 from the range of lines.

Table 14 – Gdect

№	$Gect^X_i$	$Gect^Y_i$	$Gect^\varphi_i$	№	$Gect^X_i$	$Gect^Y_i$	$Gect^\varphi_i$	№	$Gect^X_i$	$Gect^Y_i$	$Gect^\varphi_i$
1	-0.008	-0.058	0.494	7	0.215	0.106	0.155	13	-0.126	0.35	0.514
2	-0.077	0.048	0.494	8	-0.059	-0.233	0.863	14	-0.058	0.369	0.809
3	-0.053	0.082	0.989	9	0.082	0.25	0.268	15	-0.053	0.387	0.686
4	0.156	0.116	0.952	10	0.018	-0.297	0.235	16	0.058	-0.401	0.509
5	0.216	0.058	0.561	11	0.247	0.224	0.241	-	-	-	-
6	0.219	0.076	0.635	12	0.299	0.154	0.6	-	-	-	-

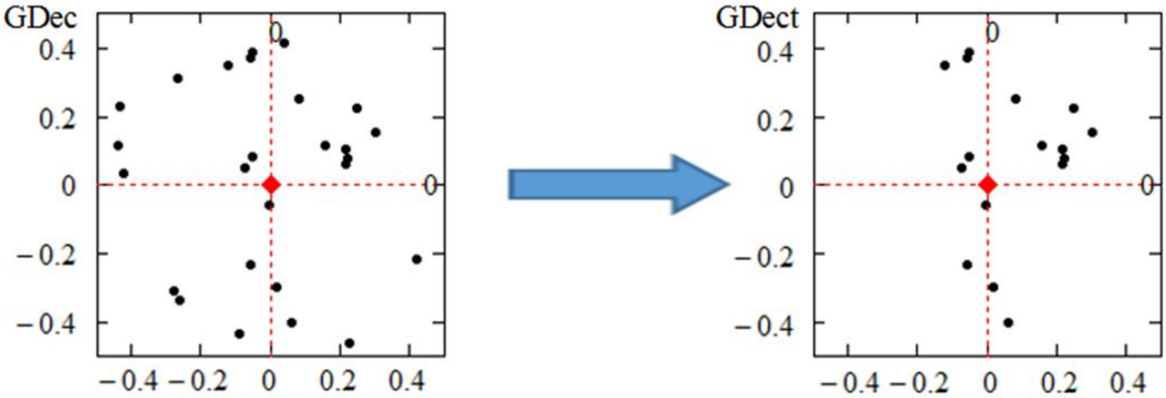

Fig. 9 – Portrait transformation after the points number limiting

Portrait position stabilization by the orientation angle on the plane

Make a portrait reversal GDect. Vector which indicates the points maximum concentration direction has to coincide with the axis O-X on the portrait plane. To do this, we define the transposed submatrix of matrix GDect:

$$XYect = \left(GDect^X, GDect^Y\right)^T. \tag{29}$$

Determine the distance of GDect portrait 16 points from the image geometric center:

$$r_i = \left|\left(XYect\right)_i\right|, \quad i = 1, \cdots, 16 \tag{30}$$

and calculate the point projection coordinates matrix on the circle located around the center:

$$XYectr_i = \left(XYect\right)_i \cdot \left(2r_i\right)^{-1}, \quad i = 1, \cdots, 16. \tag{31}$$

Direction vector of maximum concentration with points:

$$Vg = \sum_{i=1}^{16} XYectr_i = \sum_{i=1}^{16} \begin{pmatrix} XYectr_{i,1} \\ XYectr_{i,2} \end{pmatrix} = \begin{pmatrix} Vg_1 \\ Vg_2 \end{pmatrix} = \begin{pmatrix} 1.678 \\ 2.025 \end{pmatrix}. \tag{32}$$

Calculations (29) - (32) are illustrated in Fig. 10

The location of the vector Vg determines the required angle of axes rotation:

$$\gamma = \operatorname{arctg}\left(\frac{Vg_2}{Vg_1}\right) = 0.879 \ [\text{рад}] = 50.355^{o} \ [\text{град}]. \tag{33}$$

When the axes rotate by an angle the submatrix of the stabilized portrait new coordinates is determined by the expression:

$$XYectn = \left[U(\gamma) \cdot \left(XYect\right)\right]^T. \tag{34}$$

Column vector modified with rotation arrival angles:

$$GDectn^{\varphi} = \left(GDect^{\varphi} - \frac{\gamma}{2\cdot\pi}\right) \bmod 1 - \left\lfloor \left(GDect^{\varphi} - \frac{\gamma}{2\cdot\pi}\right) \bmod 1 \right\rfloor. \quad (35)$$

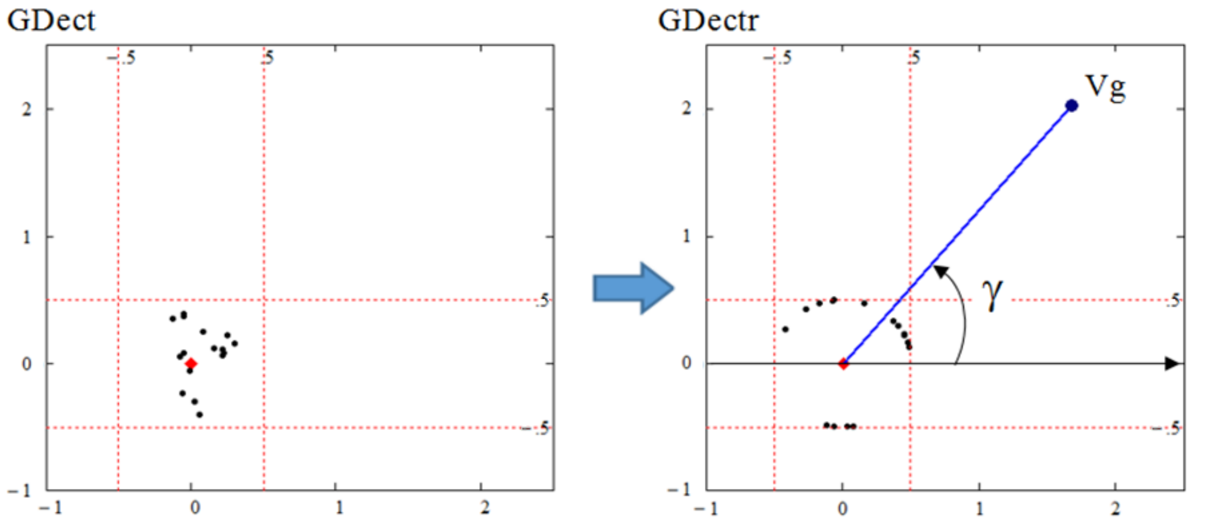

a) centered truncated portrait; *б) the points projections location on the normalized circle and direction vector of maximum concentration with points.*

Fig. 10 – Determination of the portrait angular stabilization parameters

Then the matrix of the fingerprint distorted implementation fully processed portrait will have a definition in the form:

$$GDectn = \left((XYectn) \| GDectn^{\varphi} \right). \quad (36)$$

The matrix contents are presented in table 15 and the portrait transformation with orientation angle stabilization on the plane is shown in Fig. 11.

Table 15 – Gdectn

№	$Gectn^X_i$	$Gectn^Y_i$	$Gectn^{\varphi}_i$	№	$Gectn^X_i$	$Gectn^Y_i$	$Gectn^{\varphi}_i$	№	$Gectn^X_i$	$Gectn^Y_i$	$Gectn^{\varphi}_i$
1	-0.05	-0.031	0.354	7	0.219	-0.098	0.015	13	0.189	0.32	0.375
2	-0.012	0.09	0.354	8	-0.217	-0.104	0.723	14	0.247	0.28	0.669
3	0.029	0.093	0.849	9	0.245	0.096	0.128	15	0.265	0.288	0.546
4	0.189	-0.046	0.812	10	-0.218	-0.203	0.096	16	-0.272	-0.301	0.369
5	0.182	-0.129	0.421	11	0.33	-0.047	0.101	-	-	-	-
6	0.198	-0.12	0.495	12	0.31	-0.132	0.461	-	-	-	-

The right image of fig. 11 represents the portrait final view processed according to the considered methods after the random errors action. The distorted portrait processing was carried out with the aim of distortion effect minimizing in order to approximate the characteristic points distribution to a reference sample similar distribution.

Fig. 12 shows a comparison of the distorted portrait processing result with the fingerprint obtained reference portrait normalized by the number of points and the spatial angle. Segments of straight lines indicate the distances of mutual displacement of the same points in the portraits. As we can see from the figure, in each of the portraits there is one point that does not have the corresponding pair (circled). This situation is explained by the results of the erasing and adding points processes, which are consequence of the corresponding errors.

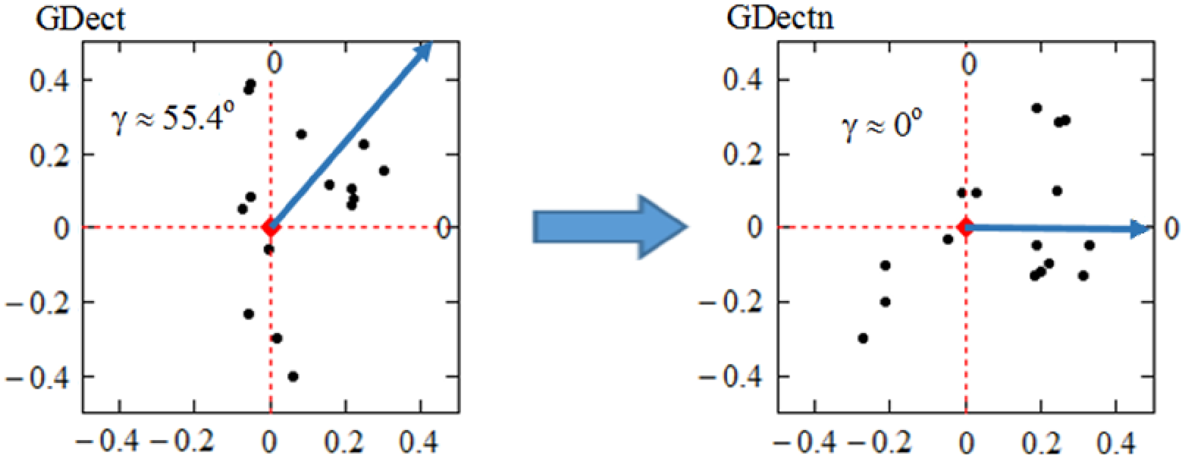

Fig. 11 – Fingerprint implementation rotation angle stabilization result

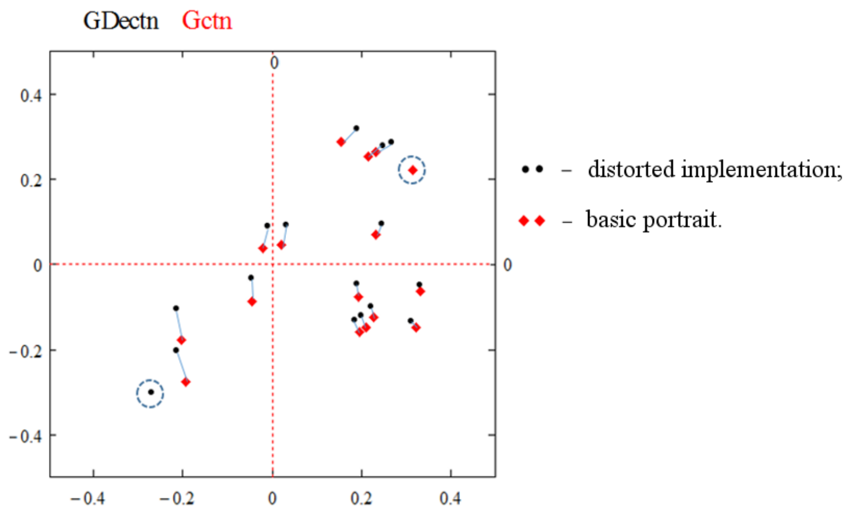

Fig. 12 – Comparison of the reference portrait points distribution with a similar distorted distribution after its processing

8 Conclusions

We have developed the mathematical models for the distorting fingerprints realizations process and for processing distorted images to minimize the random factors effect. As a result of processing the achieved value of the standard distance between the same points of the reference and processed distorted images was 4.8 % from the size of the normalized portrait square side. The proportion of points suitable for fingerprint identification by the location of the minutiae on the distorted implementation after it was processed by the proposed methods was 93.75 %.

The achieved result is characterized by a relatively high accuracy of the reference and repeated fingerprint portraits coincidence and is quite acceptable for identifying personalities based on correlation comparisons of the processed portrait with the biometric database samples. However, for the task of password access, when comparisons with standards are not permissible the indicators of high mean standard accuracy are not important. Effective secret-sharing algorithms are implemented without much difficulty if the introduced distortions do not lead to a change in the order of transferring the object characteristics (points) according to any ordered lexicographical rules. For example, from left to right and from top to bottom of the portrait square, in order of increasing distance from the center of the portrait , ascending arrival angles etc. It is obvious that even very small points displacements with respect to the reference image can cause a violation of any enumeration-listed orders.

References

[1] Rykanov A. S. Analys metodov raspoznavaniya otpechatkov pal'ca. Systemi obrabotki informacii. 2010. Vip.6. pp.164–171.
[2] Fan N. H., Spicyn V. G. Algoritmy dl'a klassifikacii otpechyatkov pal'cev na osnove primeneniya fil'tra Gabora, eyvlet-preobrazovania i mnogosloynoi neironnoy sety. Izvestia Tomskoho politechnicheskogo universiteta. Vol. 320, № 5: Upravlenie, vyichislitelnaya tehnika i informatika. pp. 60–64.
[3] Daktiloscopia.URL: http://www.ru.wikipedia.org
[4] Maltoni D., Maio D., Jain A.K., Prabhakar S. Handbook of fingerprint recognition. New York: Springer, 2003. 348 p.
[5] Zadorozhnyy V. Idenitifikacia po otpechatkam pal'cev. PC Magazine/Russian Edition. 2004. № 2. URL: http://www.bre.ru/security/20994.html
[6] Gasparyan A. V., Kyrakosyan A.A. Systema sravneniya otpechatkov pal'cev po localnym priznakam. Vestnyk RAU. Ser. fiziko-matematichaskiye i estestvennye nauki. 2006. Vip.2. pp. 85–91.
[7] Koleshko V. M., Vorobey E. A., Azizov P. M. Tradicionniye metodi biometricheskoy autentifikacii i identifikacii. Informatika cheloveka i biosistem: Uchebnoye elektronnoye izdaniye. Minsk: BNTU, 2009. 107 p.
[8] Gureeva O. Biometricheskaya identifikaciya po otpechatkam pal'cev. Tehnologiya Finger Chip. Komponentyi i tehnologii 2007. № 4. URL: http://www.kite.ru/articles/rfid/2007_4_176.php
[9] Bishop P. Atmel FingerChip Technology for Biometric Security. Atmel White Paper. URL: www.atmel.com
[10] Clarke R. Human Identification in Information Systems: Management Challenges and Public Policy Issues. Information Technology & People. 1994. Vol.7, Iss. 4. pp. 6–37 URL: https://doi.org/10.1108/09593849410076799

Рецензент: В'ячеслав Харченко, д.т.н., проф., академік Академії наук прикладної радіоелектроніки, Національний аерокосмічний університет ім. М. Є. Жуковського, м. Харків, Україна. E-mail: v_s_kharchenko@ukr.net

Надійшло: Червень 2018.

Автори:

Емілія Аніщенко, студентка кафедри Безпеки інформаційних систем і технологій, Харківський національний університет ім. В.Н. Каразіна, майдан Свободи 6, 61022, м. Харків, Україна. E-mail: emily9661@gmail.com

Сергій Рассомахін, д.т.н., зав. кафедри Безпеки інформаційних систем і технологій, Харківський національний університет ім. В. Н. Каразіна, майдан Свободи 6, 61022, м. Харків, Україна. E-mail: rassomakhin@karazin.ua

Математична модель і методи обробки біометричних зображень відбитків пальців.

Анотація. В даний час, використання технологій персональної ідентифікації на основі біометричних параметрів доступу до інформаційних ресурсів стає все більш актуальним у зв'язку з ростом інформатизації в сучасному суспільстві. Для підтвердження особи, використовуються такі фізичні характеристики, як обличчя, голос, сітківка ока або відбитки пальці. Найбільш вдалою технологією біометричної ідентифікації є порівняння відбитків пальців, завдяки простоті використання, відсутності стороннього втручання і надійності. У статті розглянута аналітична імовірнісна модель формування та обробки портретів відбитків пальців з урахуванням можливих природних факторів, здатних спотворити зображення відбитків, а також проведено деякі перетворення моделі, за допомогою яких можливо мінімізувати вплив спотворень для наближення виду розподілу характерних точок до аналогічного розподілу еталонного зразка.

Ключові слова: біометрія; модель; методи; відбитки пальців.

Рецензент: Вячеслав Харченко, д.т.н., проф., академик Академии наук прикладной радиоэлектроники, Национальный аэрокосмический университет им. М. Є. Жуковского, г. Харьков, Украина. E-mail: v_s_kharchenko@ukr.net

Поступила: Июнь 2018.

Авторы:

Емилия Анищенко, студентка кафедры Безопасности информационных систем и технологий Харьковский национальный университет им. В. Н. Каразина, пл. Свободы 6, 61022, г. Харьков, Украина. E-mail: emily9661@gmail.com

Сергей Рассомахин, д.т.н., зав. кафедры Безопасности информационных систем и технологий, Харьковский национальный университет им. В. Н. Каразина, пл. Свободы 6, 61022, г. Харьков, Украина. E-mail: rassomakhin@karazin.ua

Математическая модель и методы обработки биометрических изображений отпечатков пальцев.

Аннотация. В настоящее время, использование технологий персональной идентификации на основе биометрических параметров доступа к информационным ресурсам становится все более актуальным в связи с ростом информатизации в современном обществе. Для подтверждения личности, используются такие физические характеристики, как лицо, голос, сетчатка глаза или отпечатки пальце. Самой удачной технологией биометрической идентификации является сравнение отпечатков пальцев, благодаря простоте использования, отсутствию постороннего вмешательства и надежности. В статье рассмотрена аналитическая вероятностная модель формирования и обработки портретов отпечатков пальцев с учетом вероятных природных факторов, способных исказить изображение отпечатков, а также проведены некоторые преобразования модели, с помощью которых возможно минимизировать влияние искажений для приближения вида распределения характерных точек к аналогичному распределению эталонного образца.

Ключевые слова: биометрия; модель; методы; отпечатки пальцев.